RSC Advances

PAPER

View Article Online
View Journal | View Issue

Cite this: *RSC Adv.*, 2022, **12**, 9101

Sorption based easy-to-use low-cost filters derived from invasive weed biomass for dye contaminated water cleanup†

Smitha V. Kamath,[a] Halanur M. Manohara,[a] Kanakaraj Aruchamy,[a] Ashok Shrishail Maraddi,[a] Glenita Bridget D'Souza,[a] Kuchangi Naraseeyappa Santhosh,[a] K. N. Mahadevaprasad[a] and S. K. Nataraj *[ab]

Today, the development of functional nanostructured materials with specified morphologies utilizing environmentally friendly techniques is a very appealing topic in materials chemistry. Much emphasis has recently been paid to the utilization of biomass to make functional carbonaceous materials of varying forms, specifically carbon helices, with greater implications for the environment, economy, and society. A metal-catalyzed chemical vapour deposition technique has been developed for the fabrication of such carbon helices from nonrenewable hydrocarbons. Also, functionalization approaches were seen to necessitate high temperatures, hazardous gases, and multi-step processes. Herein, we have synthesized tendril-like functional carbon helices (HTCs) from toxic bio-weed, *Parthenium hysterophorus* as the carbon source by a greener solvothermal method employing deep eutectic solvent (DES) as both soft template and catalyst. Further, for the first time by taking advantage of the in-built chemical functionalities, HTCs were physically activated in an inert atmosphere at 900 °C (AHC) and functionalized with manganese oxide at room temperature by employing DES. Furthermore, the materials were characterized using FE-SEM, EDX, FT-IR, XRD, and BET analysis, where a surface area of 313.12 $m^2\ g^{-1}$ was achieved with a robust removal of 99.68% of methylene blue (MB) dye with a flux rate of 7432.71 LMH in a simulated continuous flow system. The obtained material was also evaluated for its specificity towards contaminant removal from an aqueous medium. Thus, Mn_3O_4/AHC membranes exhibited great promise as an easy-to-use filter for organic contaminant cleanup, with about 91% rejection of MB even at the end of the 10th cycle, indicating its potential.

Received 31st January 2022
Accepted 14th March 2022

DOI: 10.1039/d2ra00670g

rsc.li/rsc-advances

1 Introduction

Carbon nanostructures with unique physical and chemical properties have been widely studied due to their potential use in various applications like in water purification,[1] energy storage[2] and conversion devices.[3] Lately, the synthesis of carbon-based nanomaterials identified to comprise different low-dimension allotropes of carbon has been the fast-growing area of research. This includes graphite, activated carbon, carbon nanotubes, graphene, and many others.[4] These carbonaceous materials, which have been shown to display different morphological patterns (sphere, sheet-like, helical, and so on) and structural characteristics, possess unprecedented advantages due to their chemical and physical properties. One such instance was where Maria-Hormigos and group reported automotive single walled (SW)-Fe_2O_3/MnO_2 tube-shaped micromotors, whose unceasing movement was seen to impart higher adsorption efficacies and petite cleanup times. Thus, carbon nanomaterial-based micromotors with various catalytic layers made up of Pt, WO_3, TiO_2, Mg have imparted robust impact in the intended field.[5] Apart from this architecture, various other carbon nanostructures with fluorescent properties (carbon dots) along with its tunable properties and stability have been worked upon in water application for sensing of contaminants.[6] Similarly, various architectures such as scroll and ribbons have been tested with properties such as electromagnetic wave-absorption, and good adsorption efficacy towards certain contaminants.[7,8] To add on to the aforementioned properties, properties such as excellent electrical and heat conductivity, chemical stability, and high mechanical strength make these materials a priority over others.[9] On the other hand, unadorned metal oxide nanoparticles with diverse morphologies have been reported in various fields.[6–10] In the modern period, researchers are concentrating on the production of super adsorbents utilizing a variety of materials and combinations of materials, such as synthesis of nanocomposites

[a]*Centre for Nano and Material Sciences, JAIN University, Jain Global Campus, Bangalore 562112, India. E-mail: sk.nataraj@jainuniversity.ac.in; sknata@gmail.com*
[b]*IMDEA Water Institute, Avenida Punto Com, 2. Parque Científico Tecnológico de la Universidad de Alcalá, Alcalá de Henares, 28805 Madrid, Spain*

† Electronic supplementary information (ESI) available. See DOI: 10.1039/d2ra00670g

embedded with organic/inorganic materials.[10–12] Encapsulating these inorganic moieties in carbon materials like activated carbon, carbon nanotubes is likely to modify the physicochemical properties of the resulting materials.[13] The morphology and interfacial features of these materials, as well as the qualities of their constituent components, define their attributes.[14] Unfortunately, their wide practical usages are still greatly hindered despite their fascinating properties. This is mainly due to the scale-up procedures; as the laboratory scale-based batch reactor settings are quite difficult to be taken to the pilot scale, high operation cost, regeneration of the material, and recyclability issues.[15,16] Furthermore, its preparation procedure is thought to be unsustainable, resulting in large quantities of harmful by-products, raising environmental concerns.[17–19]

On the other side, the limited availability of resources has become the current motive for researchers for the development of cleaner, sustainable and environment friendly technology for wastewater purification.[20] It is clearly evident that water demand has risen significantly as a result of population growth, improved living standards, urbanization, and industry, as well as relocation of people from the countryside to urban areas in quest of better opportunities. This has led to the generation of enormous amounts of wastes that is discharged into water bodies, thereby jeopardizing aquatic life and rendering it unsuitable for domestic purposes.[21] According to reports, India, along with 33 other nations is presently experiencing its biggest water crisis in history, and 2020 was believed to be the critical year when major Indian cities were expected to run out of water.[22] In this concern, the unsustainable development goals have intended to lessen the number of individuals suffering from water related issues-either in terms of quality or quantity as one of its sixth goal.[23] Correspondingly, a study by the NITI Aayog, a government think tank, emphasized the need for "immediate and enhanced" water resource management. It has been claimed that water management is critical not just in terms of conservation, but also in terms of reclamation and reuse.[24] All of these considerations indicate the necessity for a comprehensive strategy for water resource conservation and effective management, including the smart and efficient use of water resources as well as the utilization of vast range of methods and approaches for wastewater cleanup. Till date, coagulation, ion exchange, membrane separation/filtration, photocatalysis, phytoremediation, and adsorption are examples of chemical and physical processes employed for wastewater remediation.[25–30] Amongst all, due to its simplicity and efficiency at a low cost, adsorption is the most primitive and natural technique utilized and investigated for wastewater treatment.[31–33] The most fascinating element of the adsorption process is that it has yet to be fully studied and has infinite growth potential. As a result, the development of innovative carbon-based functional materials with low-cost precursors, sustainable preparation approaches, and large-scale manufacturing capacity has recently become a critical research priority.

Thus, current research is mainly focused on using nanostructured materials which are bound to fulfil the criteria of a novel adsorbent. However, such adsorbents when used for water treatment, face problems such as leaching, recovery, which is known to reduce the efficiency of the adsorbent material and in turn may induce secondary pollution.[34] Thus, in order to overcome the above-mentioned drawbacks, the search for new synthetic strategies has recently drawn attention towards surface functionalization of the adsorbent material and assembling them into macrostructures. This is regarded to be an effective and straightforward technique for dealing with environmental issues. Their nanostructured form provides high surface area, surface-to bulk ratio and exterior functional groups that can interact with the contaminants in aqueous medium such as heavy metal ions and dyes.[35,36] These are believed to be novel functional materials in the field of biotechnology,[37,38] catalysis[39,40] as well as good adsorbents with specific selectivity for the removal of certain pollutants from wastewater[41,42] attributed to their synergistic effect. Therefore, the challenge is to prepare an adsorbent which is chemically stable, highly selective with high adsorption capacity for various chemical pollutants. In the present scientific community, abundance of opportunities exists for tuning structural and functional materials in its wide variety of raw materials including wastes from bio-origin,[43,44] carbohydrates,[45,46] and proteins.[47,48] In recent years, hybrid carbon–metal oxide heterostructures have been used in molecular sieving, adsorption, advanced oxidation processes, *etc.*[49–51] However, most of these reports involve the usage of commercially available carbon or time-consuming approaches for the preparation of functionalized carbon materials. New ideas for the design of green carbon materials have been explored and researchers are attempting to imitate biological structures to prepare promising cutting-edge materials for application in different fields.[52] Previously, our group has synthesized tendril like carbon helices from *Parthenium hysterophorus*, a lethal weed as the carbon source and the obtained material has been used for enzyme immobilization applications.[53]

In the present study, from an economic and environmental point of view, we make an attempt to functionalize the tendril-like carbon helix reported by our group[53] with Mn_xO_y and use it in powder-based membrane form for organic contaminant removal. After adsorption in a lab-scale simulated continuous-flow system, the materials were regenerated and reused for multiple cycles without much compromise in the membrane performance in terms of flux and rejection. Furthermore, the material was evaluated in terms of adsorption kinetics and isotherm studies in batch-adsorption method. Overall, the current work focusses on synthesis of Mn_xO_y functionalized helical carbon and shows how to employ it as an easy-to-use and environmentally acceptable filter for organic pollutant removal. The overall work has been schematically shown in ESI, Fig. S1.†

2 Experimental section

2.1 Materials

Parthenium hysterophorus was collected from in and around Jain University Campus, Bangalore, India. Choline chloride ($C_5H_{14}ClNO$) with percentage assay 99.0% was purchased from S.D. Fine Chemicals, Mumbai, India, anhydrous ferric chloride ($FeCl_3$) (% purity = 96.0%) from Fischer Scientific, Mumbai, India, methylene blue ($C_{16}H_{18}ClN_3S$) (dye content = 82%), methyl orange ($C_{14}H_{14}N_3NaO_3S$) (dye content ≥ 85%) was

purchased from NICE Chemicals (P) Ltd., India and used without any further purification. Whatman filter paper (grade 42) was purchased from Merck. In all of the experiments, deionized (DI) water was utilized.

2.2 Fabrication of Mn_xO_y/AHC composites

2.2.1 Synthesis of tendril-like carbon helices (HTCs). The tendril like carbon helices were synthesized by a simple solvothermal synthesis method according to our previous report.[53] Typically, leaf part of *Parthenium hysterophorus* collected was dried and ground into fine powder. The powdered biomass was added to Deep Eutectic Solvent (DES), prepared by a combination of ChoCl and $FeCl_3$ in 1 : 2 molar ratio and placed on a hot plate at 80 °C till a homogeneous mixture was obtained. To this, 50 mL of water was added. The mixture was then autoclaved in a stainless-steel Teflon lined autoclave at 200 °C for 18 hours. The product obtained from this solvothermal treatment is termed as the char. The obtained product was then filtered and washed free of impurities using distilled water; followed by washing with 1 M HCl to remove the metal ion impurities. Further washed with ethanol–water mixture in 4 : 6 weight ratio to remove ionic impurities present in the biomass. Finally, it was washed with distilled water. The as obtained hydrochar was then dried in a hot air oven at 80 °C overnight[53] and this material is designated as HTC.

2.2.2 Physical activation of HTCs. Due to the decomposition of biomass during the solvothermal treatment, the char obtained is often filled with disorganized carbon material; which in turn leads to inaccessible pores and low surface area. Thus, an activation process is required to remove the disorganized materials in order to achieve an accessible interconnected porous structure which facilitates it to be a better adsorbent. Thus, the char was subjected to physical activation in an inert atmosphere with nitrogen flow at 900 °C for 3 hours with a ramp rate of 5 °C per minute. The obtained activation carbon is designated as AHC.

2.2.3 Preparation of Mn_xO_y/AHC composites. To the obtained activated carbon, $KMnO_4$ was added in 1 : 5 weight ratio. It was then dissolved in minimum amount of water (0.076 g mL^{-1} solubility). To it, 2 mL DES (ChoCl + $FeCl_3$) was added and set aside for about an hour. The Mn_xO_y/AHC composite thus obtained, was washed free off impurities using distilled water and dried at 80 °C. The obtained oxide of manganese was found to be Mn_3O_4 by XRD.[54] The schematic synthesis of Mn_xO_y/AHC composites has been shown in detail in Fig. 1.

2.3 Instrumental characterizations

The materials were analyzed using FTIR spectroscopy on a PerkinElmer instrument between 4000 and 600 cm^{-1} for all conceivable active functional groups. Morphological characterization was carried out utilizing Scanning Electron Microscopy (SEM) with a JEOL Model-JSM7100F equipment to analyze the surface morphology. Powder X-ray diffraction (RIGAKU) was used to determine the crystallinity of the as-prepared adsorbent using Cu–K1 radiation (l.14, 1.54) at a scan rate of 3 min^{-1} and a 2θ-theta range of 5–80°. In Brunauer–Emmett–Teller (BET) studies, the specific surface area of the powder is determined by the physical adsorption of a gas on the solid's surface and measuring the quantity of adsorbate gas corresponding to a monomolecular layer on the surface. Using a Zetasizer Nano ZS light scattering device (Malvern Instruments, UK) and a He–Ne laser (633 nm, 4 mW) at 298.15 K, the zeta potential of dispersed aqueous solutions (1 mg L^{-1}) of the materials was determined. The contact angle of the powder-based membrane was measured using a sessile drop contact angle analyzer (Duravision Systems-India). A UV-visible absorption spectrophotometer, the Shimadzu UV-Vis Spectrophotometer, UV-2600, was used to determine the dye concentrations in feed and filtrate solutions.

2.4 Abatement of dyes

The anionic methyl orange (MO) dye and the cationic methylene blue (MB) dye were used as model dyes to investigate the dye adsorption efficiencies of Mn_3O_4 functionalized carbon in a dead-end filtering mode. As a support, Mn_3O_4/AHC dispersion (10 mg mL^{-1}) was filtered using Whatman filter paper (area = 3.14 cm^2). Whatman filter paper was chosen due to its ease of use, low cost, and biodegradability. Whatman filter paper is also constructed of cellulose, which provides less resistance to water

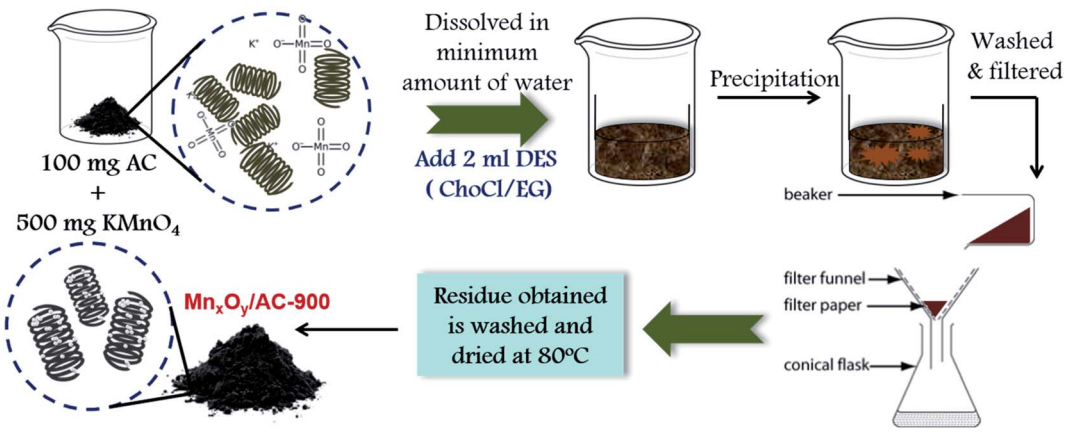

Fig. 1 Schematic for the room temperature synthesis of Mn_3O_4/AHC using deep eutectic solvent.

passage. All of the tests were done at room temperature. The continuous flow studies showed that the material was efficient in cationic dye removal. Also, flux and rejection were recorded for 20 ppm each of MB and MO dye solution (10 mL). Adsorption kinetics and isotherm studies were also carried out for the prepared adsorbent material in order to study the maximum adsorption capacity and nature of the adsorption process.

Eqn (1) was used to compute the pollutants' removal effectiveness (% R). The starting and ultimate concentrations of contaminants are represented by C_0 and C_e, respectively.[55]

$$\%R = \frac{(C_0 - C_e)}{C_0} \times 100 \quad (1)$$

Eqn (2) was used to calculate the quantity of MB uptake at equilibrium, q_e (mg g^{-1}),

$$q_e = \frac{(C_0 - C_e)}{M} \times V \quad (2)$$

where V (L) is the volume of the aqueous solution and M (g) is the mass of the dry adsorbent employed.

2.5 Regeneration studies

The reusability of Mn_3O_4/AHC was tested by executing numerous adsorption–desorption cycles to demonstrate its effectiveness. Isopropylalcohol was used as desorbing agent. The recyclability studies were executed in a continuous flow method using 10 mg Mn_3O_4/AHC material deposited in the form of powder-based membrane. MB dye solution (20 ppm/10 mL) was passed through this continuous flow setup for about ten cycles with isopropylalcohol wash (~10 mL) after every cycle.

3 Results and discussion

Parthenium hysterophorus is a common noxious plant that produces parthenin, a poisonous chemical. This toxin is known to cause dermatitis and respiratory problems in people, as well

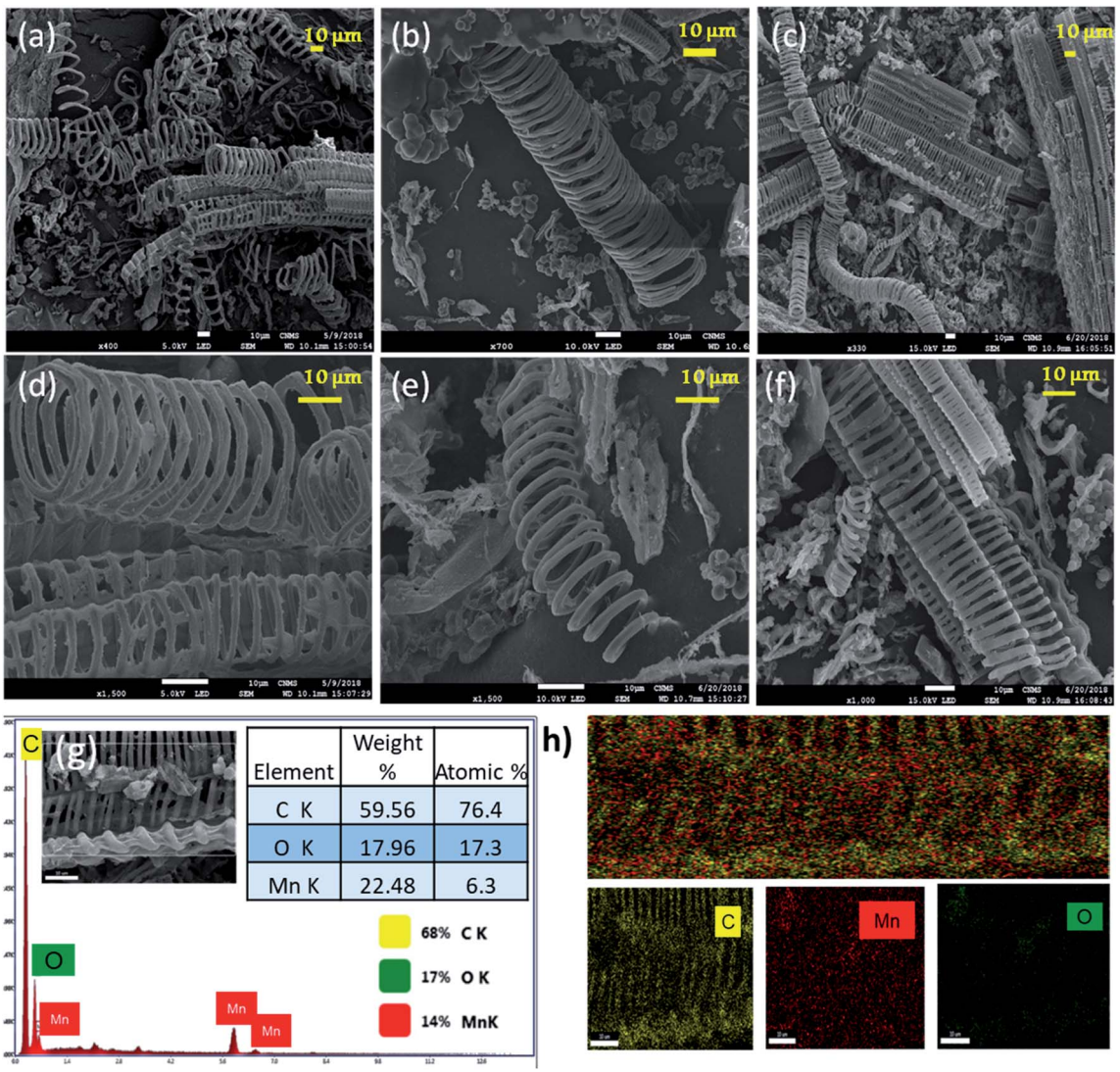

Fig. 2 FESEM micrographs of (a) and (d) HCFs obtained on solvothermal treatment. (b) and (e) HCFs physically activated at 900 °C (AHC). (c) and (f) Mn_3O_4 functionalized HCFs (Mn_3O_4/AHC). (g) and (h) Elemental mapping of Mn_3O_4 functionalized HCFs (Mn_3O_4/AHC).

as cattle and domestic animals. This invasive plant has been used as a lignocellulosic biomass precursor to create functional carbonaceous material for wastewater treatment.[53] This step has resulted in cost-effective and successful weed management. Out of the various methods employed for carbonization, from an environmental perspective, we have employed solvothermal method as reported by Kanakaraj *et al.*[53] This method of synthesis is believed to be greener due to less energy requirement and involves low temperatures of about 200 °C for a duration of 18 h. The approach used to make Mn_3O_4/AHC is shown in Fig. 1. To observe the size, shape and surface morphologies, the prepared Mn_3O_4 functionalized carbonaceous materials were analyzed using FESEM as shown in Fig. 2. Formation of tendril-like carbon helices (HTCs) with fibre width 1.5–2.0 μm, coil diameter 8–10 μm and coil length 30–50 μm was seen as expected.[53]

Tendril-like carbon helices (HTC) were obtained on solvothermal carbonization of *Parthenium hysterophorus* as seen from Fig. 2(a). Fig. 2(b) corresponds to the HTC physically activated at 900 °C (AHC) and from this it is clearly evident that the helical structure is retained even at high temperature treatment. Fig. 2(c) shows Mn_xO_y distributed over the surface of AHCs as seen from energy dispersive X-ray (EDAX) mapping in Fig. 2(d) and (e). Thus, it is observed that the overall morphology of the carbon helices remains the same in all three cases.

In addition, in order to investigate the potential functional active sites and their bonding interactions in the functional carbon material that has been created (Fig. 3(a)), FTIR analysis was carried out. The peak corresponding to O–H stretching was found at around 3446 cm^{-1} in both the curves. The stretching of aromatic C=C bonds is shown by the vibration bands at 1638 cm^{-1}, and the bending of C–H bonds is represented by the peak at 1385 cm^{-1}. Also, peaks corresponding to C–O–C was observed at around 1090 cm^{-1}. An additional peak at around 625 and 513 cm^{-1} was observed in the case of functionalized carbon material, Mn_3O_4/AHC, which was absent in case of AHC, thus confirming successful functionalization of the AHC.

Further, to examine the crystallinity and phase purity of the material, the sample was subjected to powder X-ray diffraction technique and the results are provided in Fig. 3(b). From the XRD data, it was confirmed that the majority of the peaks matched with Mn_3O_4 (JCPDS database no. 894837). Peaks at 2θ = 20.8°, 21.36°, and 27.6°, which correspond to crystalline cellulose, may be seen in the P-XRD of carbon helices generated under control circumstances. The presence of graphitic carbon is related to the primary intensity peak at 2θ = 26.6° (in both HTCs and AHC).

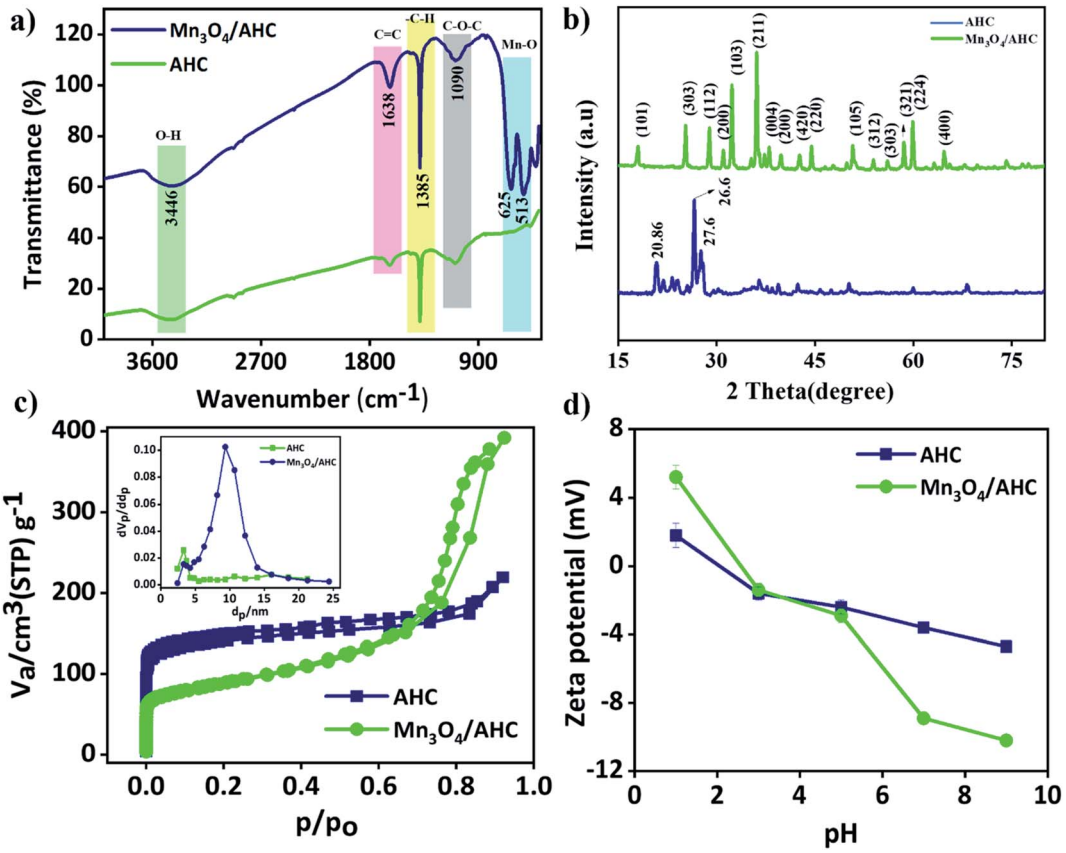

Fig. 3 (a) FTIR graph of TLCHs physically activated at 900 °C (AHC) and Mn_3O_4/AHC composite material, (b) diffraction peaks of XRD for AHC & Mn_3O_4/AHC samples. (c) BET surface area adsorption–desorption plot for the synthesized materials. Inset is a picture of pore size distribution in the as-synthesized material. (d) Surface charge trend of the synthesized materials.

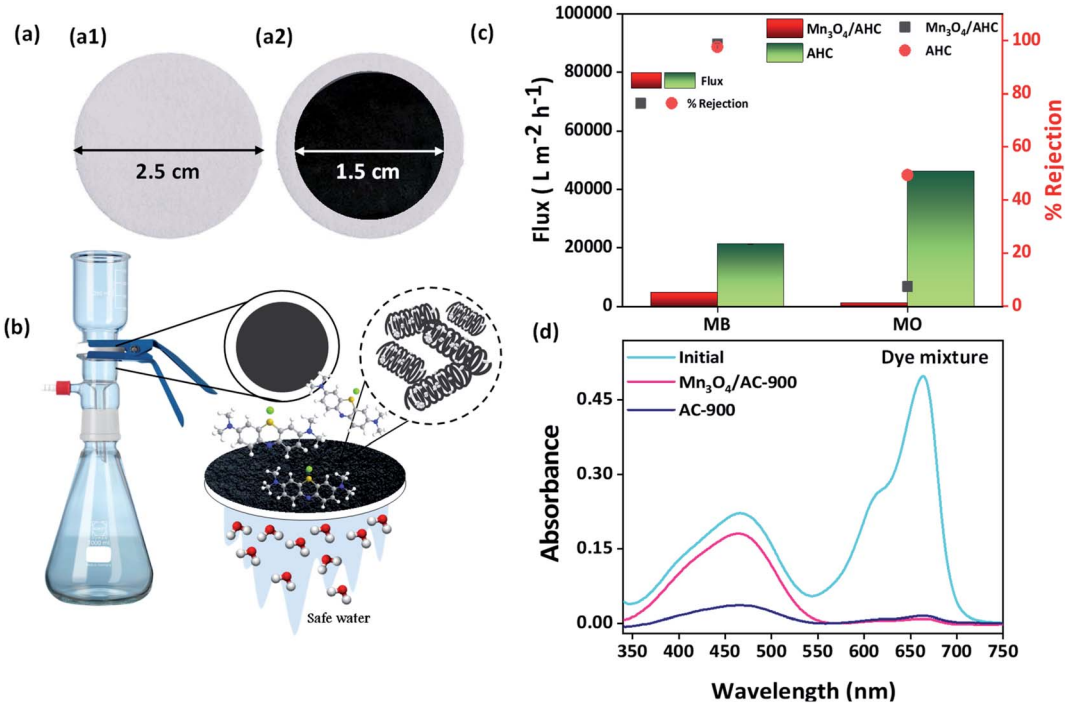

Fig. 4 Photographs of (a1) Whatman filter paper (a2) filter paper after Mn_3O_4/AHC *via* vacuum filtration. (b) Lab-scale continuous flow filtration setup for organic contaminant removal. (c) Flux and rejection for AHC and Mn_3O_4/AHC for MB and MO dyes removal *via* continuous flow and (d) UV-Vis spectra for dye mixture (MB + MO) removal using the prepared materials.

The multipoint BET was used to examine the surface area of the AHC and Mn_3O_4/AHC. Before the analysis, the materials were degassed for 2 hours at 200 °C. The control material, AHC has a specific surface area of 527.15 m^2 g^{-1} and a Type II adsorption–desorption isotherm, which is similar to that of non-porous materials. A Type IV isotherm was witnessed for Mn_3O_4/AHC with surface area, pore volume and average pore diameter of 313.12 m^2 g^{-1}, 0.6065 cm^3 g^{-1} and 7.7475 nm, respectively. The decreased surface area in the case of the active material can be attributed to the blockage of pores due to the formation of Mn_3O_4 on its surface. The zeta potential was used to compute the surface charge of AHC and Mn_3O_4/AHC. The results indicated a highly negatively charged surface in Mn_3O_4/AHC as compared to AHC with increase in pH as seen from Fig. 4(d).

3.1 Mn_3O_4/AHC – based membranes for sustainable water purification

Fabrication of Mn_3O_4/AHC materials in powder-based membrane form was used to determine the feasibility of the as prepared materials towards organic contaminant removal, as stated in the Experimental section. Contact angle measurement was used to examine the wettability of the Mn_3O_4/AHC based membrane (Fig. 6(c″)). The results indicated that the membrane has a water contact angle of 7 ± 1.4°, indicating that the membrane surface is hydrophilic. This easy-to-use filter was fabricated for the removal of cationic methylene blue, anionic methyl orange dyes and their mixtures from aqueous solutions. The photograph of the fabricated powder-based membranes is shown in Fig. 4(a). The Mn_3O_4/AHCs homogeneous coating *via*

Table 1 Results of MB, MO and dye mixture removal studies by continuous flow method[a,b]

Material	Dye	Mol. weight (g mol^{-1})	Conc. (ppm)	Analyte charge	Λ_{max} (nm)	Flux (Lm^{-2} h^{-1})	Rejection (%)
AHC	MB	319.85	20	+	663	29 829.9 ± 9.12	97.41 ± 1.66
	MO	696.66	20	−	464	15 429 ± 18.58	49.87 ± 0.98
	MB + MO	—	20			21 281.7 ± 9.12	97.28 ± 0.57
							58.87 ± 0.47
Mn_3O_4/AHC	MB	319.85	20	+	663	7432.71 ± 10.44	99.68 ± 0.88
	MO	696.66	20	−	464	1227.57 ± 5.06	7.82 ± 0.770
	MB + MO	—	20			4804.8 ± 10.44	98.49 ± 1.27
							13.05 ± 1.47

[a] Pure water flux for AHC = 30 213.02 ± 19.58 LMH. [b] Pure water flux for Mn_3O_4/AHC = 9345.45 ± 10.31 LMH.

vacuum filtration on Whatman filter paper created an excellent blockade for organic contaminants, allowing for their efficient removal. Experiments were conducted for both anionic methyl orange (MO) and cationic methylene blue (MB) as model dyes to assess the nature of active surfaces on the functionalized helical carbon adsorbent (Mn_3O_4/AHC) and the control material (AHC). A lab-scale simulated continuous-flow system as depicted in Fig. 4(b) showed a removal efficiency up to ~97.41% using unmodified activated HTC (AHC) for MB dye from the aqueous medium, whereas about 49.87% removal efficiency was observed for MO removal with flux of 29 829.9 LMH and 15 429 LMH respectively. Further, Mn_3O_4 functionalized helical carbon adsorbent (Mn_3O_4/AHC) has shown ~99.68% rejection with flux 7432.71 LMH and ~7.82% removal efficiency with flux of 1227.57 LMH for MB and MO removal (Fig. 4(c)) respectively as shown in Table 1. Also, the adsorption efficiency of Whatman

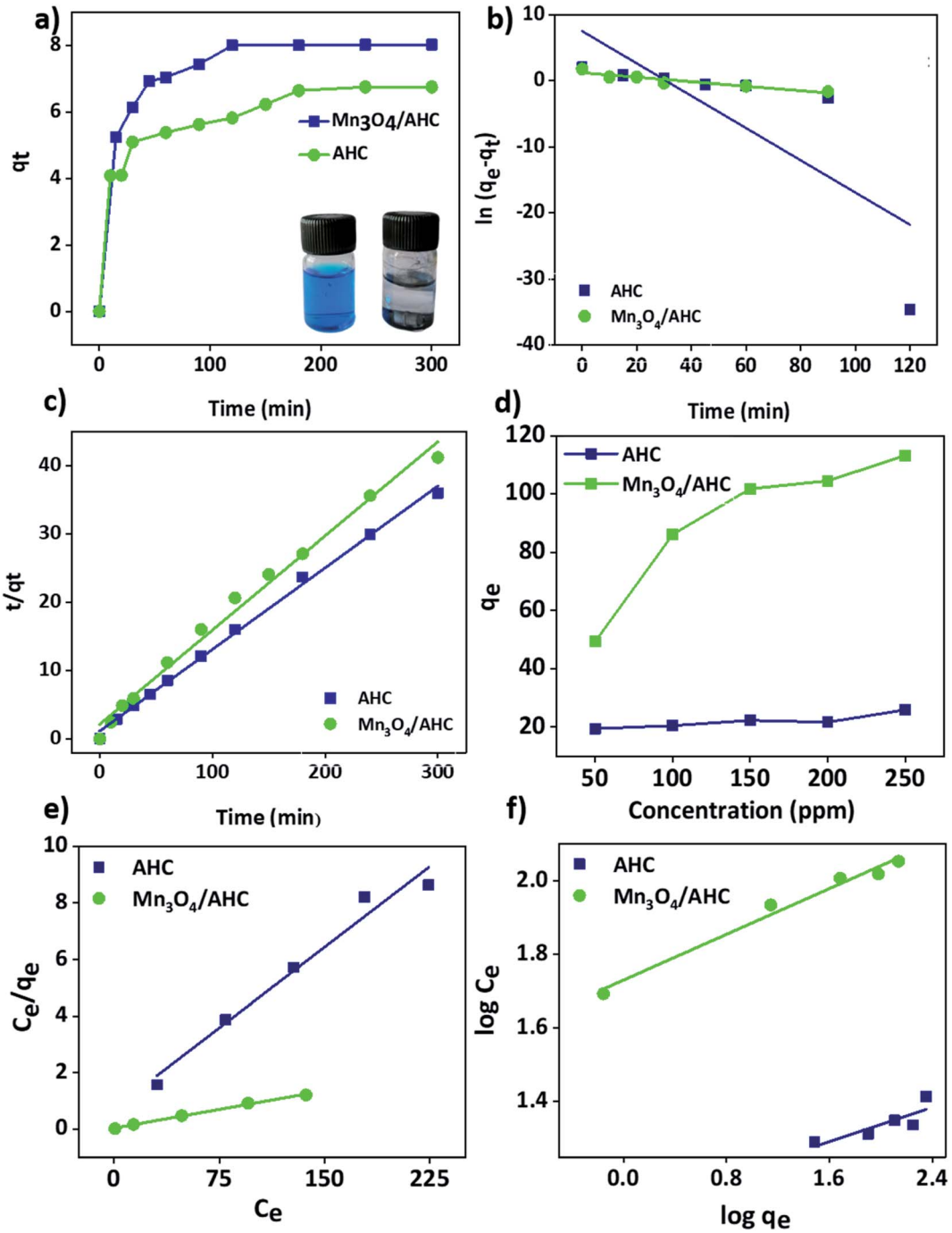

Fig. 5 (a) Effect of contact time on MB removal. Adsorption kinetics studies for MB removal (b) pseudo-first-order and (c) pseudo-second-order kinetic plots. (d) Effect of MB concentration on adsorption. Adsorption isotherm studies for MB removal (e) Freundlich isotherms and (f) Langmuir isotherms for both AHC and Mn_3O_4/AHC.

filter paper was evaluated for the removal of 20 ppm/10 mL methylene blue solution. It was calculated that the bare filter paper showed a rejection of around 8% as seen from Fig. S2.†

The above materials were also checked for their ability to selectively adsorb dyes from mixture of cationic and anionic dyes (MB + MO). From the continuous flow studies carried out for dye mixtures, it was observed that the control material (AHC) exhibited a rejection of 97% for MB and 58.87% for MO dyes from the dye mixture with a flux of 21 281.78 LMH. On the other hand, Mn_3O_4/AHC showed selective adsorption of MB over MO with a rejection of 99.49% for MB and 13% for MO, achieving a flux of 4804.8 LMH. From the experiments run, it was evident that the Mn_3O_4 functionalized carbon adsorbent had greater affinity towards the cationic dye than the anionic attributing to the negative charge imparted by the oxygenated functionalities present in the solvothermally prepared starting material. The UV-Vis spectra for MB and MO before and after adsorption with Mn_3O_4/AHC and AHC are given in Fig. 4(d).

3.2 Batch adsorption studies

To investigate the nature (physical or chemical) and rate of adsorption, adsorption dynamics for the process were studied. As seen from plot 5(a) the effect of contact time on MB dye adsorption indicated that for both AHC and Mn_3O_4/AHC, the percentage adsorption increased as contact time increased. The plot revealed that most of the adsorption took place within 90–100 minutes; after which, there was no much dye adsorption for both AHC or Mn_3O_4/AHC. At room temperature, 20 mL MB solution (50 mg L^{-1}) and 0.01 g of the adsorbent material were used to conduct kinetic studies for MB removal utilizing the Mn_3O_4 functionalized carbon and the control material. Also, varied concentrations of MB were taken by keeping the amount of adsorbent constant (0.01 g). The results showed that due to the accessible adsorption sites on the adsorbent materials at low MB concentrations, all of the MB molecules adhered to the available sites. However, when the concentration of MB in the solution rose, adsorption reduced due to filling of the accessible adsorption sites on the adsorbent material. This pattern is evident from Fig. 5(d). Adsorption isotherm studies were carried out in order to study the design of the adsorption process. From Fig. 5(b) and (c) the linear regression correlations (R^2) for pseudo-first-order model were found to be lower than those of pseudo-second-order model for MB dye removal. The calculated correlation coefficient R^2 for pseudo-second-order model was much closer to unity (>0.9) exhibited from both AHC and Mn_3O_4/AHC materials. Therefore, the adsorption experiments run shows an inclination towards monolayer adsorption and indicated that the rate of adsorption was found to depend only on the adsorption capacity of the prepared adsorbent material and not on the concentration of the contaminants. Adsorption isotherms were explored using two commonly used isotherm models, the Langmuir model and the Freundlich model, to better study the interplay between adsorbent–adsorbate and the adsorption capacity (Fig. 5(e) and (f)). The Langmuir model has a greater correlation coefficient than the Freundlich model, showing that MB adsorption on adsorbents is based on monolayer adsorption and the presence of homogeneous active sites on the adsorbents. We have achieved a maximum adsorption capacity of 26.23 mg g^{-1} or the control material, AHC and for Mn_3O_4/AHC is 113.37 mg g^{-1} (ESI, Tables S1 and S2†).

3.3 Recyclability studies

In recent years, the regeneration and disposal of waste adsorbents have been extensively debated in order to certify their recycling and limit the possible hazards of waste adsorbents. In general, incorrect disposal of used adsorbents can result in

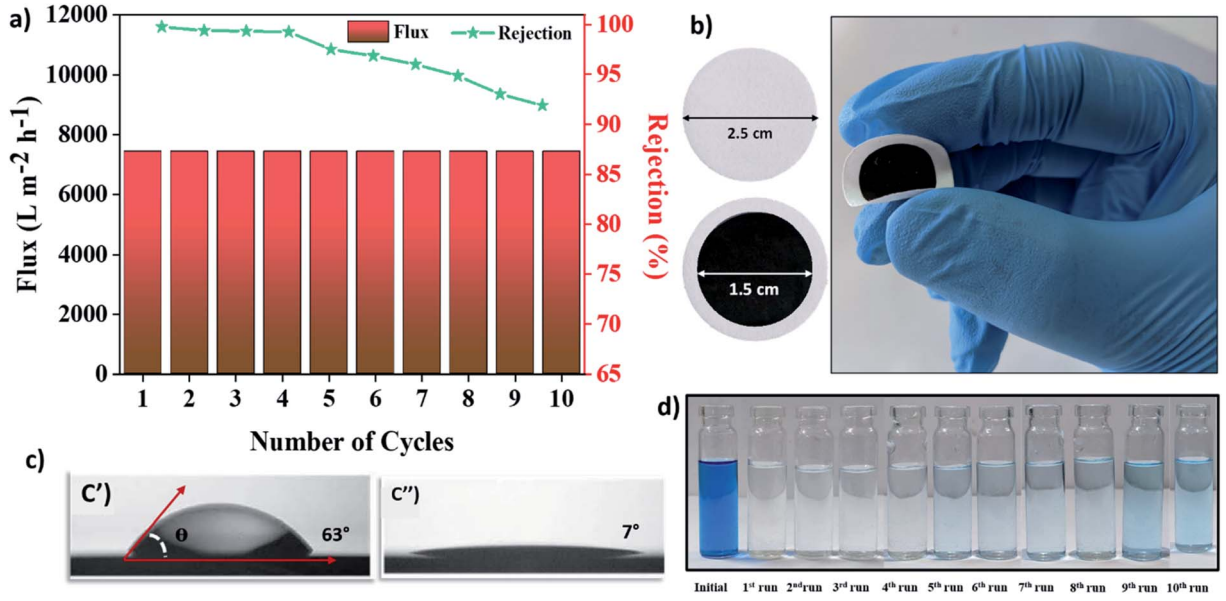

Fig. 6 (a) Regeneration study of Mn_3O_4/AHC for adsorption of MB dye. (b) Photograph of Mn_3O_4/AHC powder-based membrane. (c) Contact angle measurements for the prepared membranes. (c′) AHC membrane, (c″) Mn_3O_4/AHC membrane. (d) Digital photograph of permeates obtained during the recyclability study.

significant environmental issues. Therefore, an important part of any study is the regeneration and reuse of the material as a step towards solid waste management and to improve the economy of wastewater purification phenomena. An attempt was made in this work as well to renew the membrane active sites and utilize them for further filtering. The materials were effectively renewed using isopropylalcohol. The material was recycled without much compromise in flux and adsorption capacity. For ten consecutive cycles, there was a steady drop in rejection from ~99% to ~91%. The slight decrease in performance might be due to unrecovered MB from the material's surface even after sonication (Fig. 6). Nonetheless, a membrane's performance is considered to be superior if it rejects >90 percent even after the tenth cycle. Thus, demonstrating the Mn_3O_4/AHC composite's regeneration potential. As a result, the Mn_3O_4/AHC composite might be a promising and cost-effective adsorbent for the abatement of MB molecules polluted wastewater.

4 Conclusion

In summary, a robust Mn_3O_4/AHC composite with adsorption capacity of 113 mg g^{-1} has been synthesized, with improved surface functionalities and a moderate surface area of 313.12 m^2 g^{-1} with helical morphology *via* a simple and lucrative solvothermal method. This material was then fabricated into a powder-based membrane form *via* vacuum deposition method; which can be used in a dead-end filtration mode for contaminant removal. Methylene blue dyes were efficaciously removed from aqueous medium using the as fabricated Mn_3O_4/AHC membranes. The prepared membranes exhibited an extraordinary flux rate of 7432.71 LMH and high rejection of about 99.68%. Nearly 7.82% removal efficiency with a flux of 1227.57 LMH was recorded for anionic methyl orange dye. Experiments run for the mixture of anionic and cationic dyes revealed the selectiveness of the membrane towards cationic contaminants. Besides, the used Mn_3O_4/AHC membranes were recycled upto 10 cycles for MB removal without significant compromise in its efficacy. In conclusion, the current research has produced a scalable and ecologically friendly Mn_3O_4/AHC based membrane filtering technique that may be employed as an easy-to-use dye abatement filter.

Author contributions

The idea was conceptualized by SKN, who also devised the tests. SVK carried out all of the experiments and prepared the paper. MHM and AK assisted with data analysis. Data and characterizations were collected with the help of ASM, GBD, KNS, and KNM.

Conflicts of interest

The authors state that they have no known competing financial interests or personal ties that may have influenced the work presented in this study.

Acknowledgements

SKN thanks the Department of Science and Technology of the Government of India for the DST-Nanomission Project (SR/NM/NT1073/2016), the DST-Technology Mission Project (DST/TMD/HFC/2K18/124G) of the Government of India, and the Talent Attraction Program funded by the Community of Madrid, Spain (2017-T1/AMB5610), as well as the Government of India for the DST-INSPIRE Fellowship, Grant #IFA12.

References

1 B. Luo, G. Huang, Y. Yao, C. An, P. Zhang and K. Zhao, Investigation into the influencing factors and adsorption characteristics in the removal of sulfonamide antibiotics by carbonaceous materials, *J. Cleaner Prod.*, 2021, **319**, 128692.
2 J. Islam, F. I. Chowdhury, J. Uddin, R. Amin and J. Uddin, Review on carbonaceous materials and metal composites in deformable electrodes for flexible lithium-ion batteries, *RSC Adv.*, 2021, **11**(11), 5958–5992.
3 M. Giorcelli, M. Bartoli, A. Sanginario, E. Padovano, C. Rosso, M. Rovere and A. Tagliaferro, High-Temperature Annealed Biochar as a Conductive Filler for the Production of Piezoresistive Materials for Energy Conversion Application, *ACS Appl. Electron. Mater.*, 2021, **3**(2), 838–844.
4 R. Gusain, N. Kumar and S. S. Ray, Recent advances in carbon nanomaterial-based adsorbents for water purification, *Coord. Chem. Rev.*, 2020, **405**, 213111.
5 R. Maria-Hormigos, M. Pacheco, B. Jurado-Sánchez and A. Escarpa, Carbon nanotubes-ferrite-manganese dioxide micromotors for advanced oxidation processes in water treatment, *Environ. Sci.: Nano*, 2018, **5**(12), 2993–3003.
6 N. K. R. Bogireddy, J. Lara, L. R. Fragoso and V. Agarwal, One-step hydrothermal preparation of highly stable N doped oxidized carbon dots for toxic organic pollutants sensing and bioimaging, *Chem. Eng. J.*, 2020, **401**, 126097.
7 P. K. Samantaray, S. Baloda, G. Madras and S. Bose, Nanodelivery in scrolls-based nanocarriers: efficient constructs for sustainable scavenging of heavy metal ions and inactivate bacteria, *ACS Sustainable Chem. Eng.*, 2019, **7**(23), 18775–18784.
8 L. Huang, Z.-h. Yang, L.-j. Yan, S. I. Alhassan, H.-y. Gang, W. Ting and H.-y. Wang, Preparation of 2D carbon ribbon/Al_2O_3 and nitrogen-doped carbon ribbon/Al_2O_3 by using MOFs as precursors for removing high-fluoride water, *Trans. Nonferrous Met. Soc. China*, 2021, **31**(7), 2174–2188.
9 Y. Gong, H. Wang, Z. Wei, L. Xie and Y. Wang, Engineering, an efficient way to introduce hierarchical structure into biomass-based hydrothermal carbonaceous materials, *ACS Sustainable Chem. Eng.*, 2014, **2**(10), 2435–2441.
10 Y. Deng, G.-L. Song, D. Zheng and Y. Zhang, Fabrication and synergistic antibacterial and antifouling effect of an organic/inorganic hybrid coating embedded with nanocomposite Ag@TA-SiO_2 particles, *Colloids Surf., A*, 2021, **613**, 126085.
11 F. B. Ajdari, E. Kowsari, M. N. Shahrak, A. Ehsani, Z. Kiaei, H. Torkzaban, M. Ershadi, S. K. Eshkalak, V. Haddadi-Asl and A. Chinnappan, A review on the field patents and

recent developments over the application of metal organic frameworks (MOFs) in supercapacitors, *Coord. Chem. Rev.*, 2020, **422**, 213441.

12 I. Topolniak, *Novel boehmite-embedded organic/inorganic hybrid nanocomposite: cure behaviour, morphology and thermal properties*, 2018.

13 R. Dubey, D. Dutta, A. Sarkar and P. Chattopadhyay, Functionalized Carbon Nanotubes: Synthesis, Properties and Applications in Water Purification, Drug Delivery, Material and Biomedical Science, *Nanoscale Adv.*, 2021, 5722–5744.

14 B. Hashemi and S. Rezania, Carbon-based sorbents and their nanocomposites for the enrichment of heavy metal ions: a review, *Microchim. Acta*, 2019, **186**(8), 1–20.

15 X. Qu, J. Brame, Q. Li and P. J. Alvarez, Nanotechnology for a safe and sustainable water supply: enabling integrated water treatment and reuse, *Acc. Chem. Res.*, 2013, **46**(3), 834–843.

16 P. J. Alvarez, C. K. Chan, M. Elimelech, N. J. Halas and D. Villagrán, Emerging opportunities for nanotechnology to enhance water security, *Nat. Nanotechnol.*, 2018, **13**(8), 634–641.

17 E.-X. Ding, J. Wang, H.-Z. Geng, W.-Y. Wang, Y. Wang, Z.-C. Zhang, Z.-J. Luo, H.-J. Yang, C.-X. Zou and J. Kang, Y-junction carbon nanocoils: synthesis by chemical vapor deposition and formation mechanism, *Sci. Rep.*, 2015, **5**(1), 1–9.

18 A. Shaikjee and N. J. Coville, The synthesis, properties and uses of carbon materials with helical morphology, *J. Adv. Res.*, 2012, **3**(3), 195–223.

19 W.-C. Liu, H.-K. Lin, Y.-L. Chen, C.-Y. Lee and H.-T. Chiu, Growth of carbon nanocoils from K and Ag cooperative bicatalyst assisted thermal decomposition of acetylene, *ACS Nano*, 2010, **4**(7), 4149–4157.

20 S. H. Khan, Green nanotechnology for the environment and sustainable development, In *Green materials for wastewater treatment*, Springer, 2020, pp. 13–46.

21 J. Sudarsan, S. Vaishampayan and V. Srihari, Grey water recycling as a tangible solution to water crisis: a case study in Thiruvananthapuram, India, *International Journal of Energy Water Resources*, 2021, **5**(4), 441–445.

22 N. Paul and L. Elango, Predicting future water supply-demand gap with a new reservoir, desalination plant and waste water reuse by water evaluation and planning model for Chennai megacity, India, *Groundw. Sustain. Dev.*, 2018, **7**, 8–19.

23 G. Assembly, *Sustainable development goals, SDGs Transform Our World, 2030*, 2015.

24 K. Singh and S. Mahanta, Sustainable Urban Water Management Strategies, In *Water Governance and Management in India*, Springer, 2021; pp. 23–43.

25 R. N. Maalige, K. Aruchamy, A. Mahto, V. Sharma, D. Deepika, D. Mondal and S. K. Nataraj, Low operating pressure nanofiltration membrane with functionalized natural nanoclay as antifouling and flux promoting agent, *Chem. Eng. J.*, 2019, **358**, 821–830.

26 T. Leiknes, The effect of coupling coagulation and flocculation with membrane filtration in water treatment: a review, *J. Environ. Sci.*, 2009, **21**(1), 8–12.

27 M. Edgar and T. H. Boyer, Removal of natural organic matter by ion exchange: comparing regenerated and non-regenerated columns, *Water Res.*, 2021, **189**, 116661.

28 G. Ren, H. Han, Y. Wang, S. Liu, J. Zhao, X. Meng and Z. Li, Recent advances of photocatalytic application in water treatment: a review, *Nanomaterials*, 2021, **11**(7), 1804.

29 H. M. Mustafa and G. Hayder, Recent studies on applications of aquatic weed plants in phytoremediation of wastewater: a review article, *Ain Shams Eng. J.*, 2021, **12**(1), 355–365.

30 F. Karimi, A. Ayati, B. Tanhaei, A. L. Sanati, S. Afshar, A. Kardan, Z. Dabirifar and C. Karaman, Removal of metal ions using a new magnetic chitosan nano-bio-adsorbent; a powerful approach in water treatment, *Environ. Res.*, 2022, **203**, 111753.

31 W. Gu, X. Huang, Y. Tian, M. Cao, L. Zhou, Y. Zhou, J. Lu, J. Lei, Y. Zhou and L. Wang, High-efficiency adsorption of tetracycline by cooperation of carbon and iron in a magnetic Fe/porous carbon hybrid with effective Fenton regeneration, *Appl. Surf. Sci.*, 2021, **538**, 147813.

32 M. Sharma, M. Joshi, S. Nigam, S. Shree, D. K. Avasthi, R. Adelung, S. K. Srivastava and Y. K. Mishra, ZnO tetrapods and activated carbon based hybrid composite: adsorbents for enhanced decontamination of hexavalent chromium from aqueous solution, *Chem. Eng. J.*, 2019, **358**, 540–551.

33 G. Cheng, F. Xu, J. Xiong, F. Tian, J. Ding, F. J. Stadler and R. Chen, Enhanced adsorption and photocatalysis capability of generally synthesized TiO_2-carbon materials hybrids, *Adv. Powder Technol.*, 2016, **27**(5), 1949–1962.

34 S. Lata and S. Samadder, Removal of arsenic from water using nano adsorbents and challenges: a review, *J. Environ. Manage.*, 2016, **166**, 387–406.

35 A. Jawed, V. Saxena and L. M. Pandey, Engineered nanomaterials and their surface functionalization for the removal of heavy metals: a review, *J. Water Process. Eng.*, 2020, **33**, 101009.

36 M. Manyangadze, N. Chikuruwo, C. Chakra, T. Narsaiah, M. Radhakumari and G. Danha, Enhancing adsorption capacity of nano-adsorbents *via* surface modification: a review, *S. Afr. J. Chem. Eng.*, 2020, **31**(1), 25–32.

37 S. P. Schwaminger, P. Fraga-García, M. Eigenfeld, T. M. Becker and S. Berensmeier, Magnetic separation in bioprocessing beyond the analytical scale: from biotechnology to the food industry, *Front. Bioeng. Biotechnol.*, 2019, **7**, 233.

38 Z. Chen, Z. Lv, Y. Sun, Z. Chi and G. Qing, Recent advancements in polyethyleneimine-based materials and their biomedical, biotechnology, and biomaterial applications, *J. Mater. Chem.*, 2020, **8**(15), 2951–2973.

39 Y. Fu, Y. Sun, Z. Chen, S. Ying, J. Wang and J. Hu, Functionalized magnetic mesoporous silica/poly(*m*-aminothiophenol) nanocomposite for Hg(II) rapid uptake

and high catalytic activity of spent Hg(II) adsorbent, *Sci. Total Environ.*, 2019, **691**, 664–674.

40 K. Cui, B. Yan, Y. Xie, H. Qian, X. Wang, Q. Huang, Y. He, S. Jin and H. Zeng, Regenerable urchin-like Fe_3O_4@PDA-Ag hollow microspheres as catalyst and adsorbent for enhanced removal of organic dyes, *J. Hazard. Mater.*, 2018, **350**, 66–75.

41 Y. Hua, J. Xiao, Q. Zhang, C. Cui and C. Wang, Facile synthesis of surface-functionalized magnetic nanocomposites for effectively selective adsorption of cationic dyes, *Nanoscale Res. Lett.*, 2018, **13**(1), 1–9.

42 L. Li, Y. Xu, D. Zhong and N. Zhong, CTAB-surface-functionalized magnetic MOF@MOF composite adsorbent for Cr(VI) efficient removal from aqueous solution, *Colloids Surf., A*, 2020, **586**, 124255.

43 W. C. Moon, A review on interesting properties of chicken feather as low-cost adsorbent, *Int. J. Integr. Eng.*, 2019, **11**(2), 136–146.

44 C. K. Jain, D. S. Malik and A. K. Yadav, Applicability of plant based biosorbents in the removal of heavy metals: a review, *Environ. Processes*, 2016, **3**(2), 495–523.

45 Y. Li, S. Wang, B. Wang, Y. Wang and J. Wei, Sustainable biomass glucose-derived porous carbon spheres with high nitrogen doping: as a promising adsorbent for $CO_2/CH_4/N_2$ adsorptive separation, *Nanomaterials*, 2020, **10**(1), 174.

46 V. T. Sharma, S. V. Kamath, D. Mondal and N. S. Kotrappanavar, Fe–Al based nanocomposite reinforced hydrothermal carbon: efficient and robust absorbent for anionic dyes, *Chemosphere*, 2020, **259**, 127421.

47 J. Yu, Y. Kang, W. Yin, J. Fan and Z. Guo, Removal of antibiotics from aqueous solutions by a carbon adsorbent derived from protein-waste-doped biomass, *ACS Omega*, 2020, **5**(30), 19187–19193.

48 J. Carvalho, J. Araújo and F. Castro, Alternative low-cost adsorbent for water and wastewater decontamination derived from eggshell waste: an overview, *Waste Biomass Valorization*, 2011, **2**(2), 157–167.

49 Y. Li, Q. Du, J. Wang, T. Liu, J. Sun, Y. Wang, Z. Wang, Y. Xia and L. Xia, Defluoridation from aqueous solution by manganese oxide coated graphene oxide, *J. Fluorine Chem.*, 2013, **148**, 67–73.

50 C. Luo, R. Wei, D. Guo, S. Zhang and S. Yan, Adsorption behavior of MnO_2 functionalized multi-walled carbon nanotubes for the removal of cadmium from aqueous solutions, *Chem. Eng. J.*, 2013, **225**, 406–415.

51 Y. Li, M. Xia, F. An, N. Ma, X. Jiang, S. Zhu, D. Wang and J. Ma, Superior removal of Hg(II) ions from wastewater using hierarchically porous, functionalized carbon, *J. Hazard. Mater.*, 2019, **371**, 33–41.

52 W. Wang, A. Saeed, J. He, Z. Wang, D. Zhan, Z. Li, C. Wang, Y. Sun, F. Tao and W. Xu, Bio-inspired porous helical carbon fibers with ultrahigh specific surface area for super-efficient removal of sulfamethoxazole from water, *J. Colloid Interface Sci.*, 2020, **578**, 304–314.

53 K. Aruchamy, M. Bisht, P. Venkatesu, D. Kalpana, M. Nidhi, N. Singh, D. Ghosh, D. Mondal and S. K. Nataraj, Direct conversion of lignocellulosic biomass to biomimetic tendril-like functional carbon helices: a protein friendly host for cytochrome C, *Green Chem.*, 2018, **20**(16), 3711–3716.

54 K. Aruchamy, A. Mahto, R. Nagaraj, D. Kalpana, D. Ghosh, D. Mondal and S. K. Nataraj, Ultrafast synthesis of exfoliated manganese oxides in deep eutectic solvents for water purification and energy storage, *Chem. Eng. J.*, 2020, **379**, 122327.

55 H. M. Manohara, K. Aruchamy, S. Chakraborty, N. Radha, M. R. Nidhi, D. Ghosh, S. K. Nataraj and D. Mondal, Sustainable water purification using an engineered solvothermal carbon based membrane derived from a eutectic system, *ACS Sustainable Chem. Eng.*, 2019, **7**(11), 10143–10153.